Pressure-induced ion pairing in MgSO$_4$ solutions: Implications for the oceans of icy worlds

C. Schmidt[1]*, C.E. Manning[2]

Abstract

At ambient temperature, liquid water transforms from a low-density to a high-density dynamic structure at ~0.2 GPa. The transition persists in electrolyte solutions; however, its effects on solute properties are unknown. We obtained Raman spectra of 0.5–2.0 molal MgSO$_4$ solutions at 21 °C and 10^{-4} to ~1.6 GPa. Above about 0.4 GPa, we observed an increase in the MgSO$_4$ contact ion pair abundance with pressure, regardless of concentration. This phenomenon contravenes the general rule that dissolved salts dissociate upon compression, and is likely caused by the structural collapse in the solvent with pressure due to increased hydrogen-bond breaking. Increasing ion association in high-pressure aqueous solutions implies that, at a given salinity, high-density water in deep, cold planetary oceans and pore waters will possess lower ionic strength and electric conductivity than previously thought. This behaviour will also lead to higher ocean salinity in the interiors of Pluto and the largest icy moons of Jupiter and Saturn, Ganymede, Callisto, and Titan, or in exoplanet water-worlds, through enhancement of submarine silicate weathering.

Introduction

The physical properties of liquid water at ambient temperature consistently display anomalous behaviour upon compression to densities of ~1.1 g cm^{-3}. These include *e.g.*, radial distribution functions from X-ray scattering (Okhulkov *et al.*, 1994) and neutron diffraction (Soper and Ricci, 2000), a distinct anomaly in the high-frequency sound velocity from inelastic X-ray scattering experiments (Krisch *et al.*, 2002), the Raman shift of the O–H stretching vibration (Kawamoto *et al.*, 2004), the sound velocity from Brillouin spectroscopy (Li *et al.*, 2005),

1. Deutsches GeoForschungsZentrum (GFZ), Section 4.3 Chemistry and Physics of Earth Materials, Telegrafenberg, 14473 Potsdam, Germany
* Corresponding author (email: Christian.Schmidt@gfz-potsdam.de)
2. Department of Earth, Planetary, and Space Sciences, University of California, Los Angeles, CA 90025-1567, USA

and the isothermal compressibility (Mirwald, 2005). The experiments indicate a transition from an open structure in low-density water (LDW) to a structure with a collapsed second coordination shell in high-density water (HDW) (Soper and Ricci, 2000). Based on femtosecond infrared pump-probe spectroscopy on a D$_2$O-H$_2$O mixture, the LDW-HDW transition is at ~0.25 GPa at 273 K and ~0.2 GPa at 298 K, but not observed at 363 K (Fanetti *et al.*, 2014).

Dissolved salts also disrupt the hydrogen-bonded dynamic H$_2$O structure due to formation of hydration shells around the ions. It is not clear if, and by how much, the structure outside the first hydration shell is affected (Marcus, 2009), but there is considerable evidence that the LDW-HDW transition persists in saline solutions even at fairly high solute concentrations (Mirwald, 2005; Schmidt, 2009; Valenti *et al.*, 2012). However, the effects of the transition on solute-solute interactions have not been investigated. Here, we studied the pressure-dependent variation in contact ion pairing in MgSO$_4$ solutions at 21 °C over a large range in pressure across the LDW-HDW transition until the sample solidified upon compression. We used MgSO$_4$ solutions because they are thought to be important components of planetary oceans (Zolotov and Shock, 2001) and because Raman scattering from the symmetric stretching vibration of sulphate (ν_1-SO$_4^{2-}$) provides direct information about the fraction of contact ion pairs.

Compression-Enhanced Contact Ion Pairing

At all conditions, the Raman band shape in the ν_1-SO$_4^{2-}$ region was accurately described using two Gaussian + Lorentzian components (Fig. S-1a). The higher wavenumber component is assigned to contact ion pairs Mg^{2+}SO$_4^{2-}$(aq) (CIP), and the lower wavenumber component, here designated SO$_4$*, includes Raman-indistinguishable contributions from unassociated SO$_4^{2-}$(aq) ions, solvent-shared ion pairs Mg^{2+}(OH$_2$)SO$_4^{2-}$(aq) (SIP), and double solvent-separated ion pairs Mg^{2+}(OH$_2$)$_2$SO$_4^{2-}$(aq) (2SIP) (Rudolph *et al.*, 2003). Spectra in the O–H stretching region were recorded for the 2.0 molal solution. A three component model yielded good fits with internally consistent results for all spectra (Fig. S-1b). We assign the components C2 and C3 at ~3450 cm^{-1} and ~3580 cm^{-1} to ν_1 and ν_3 of H$_2$O monomers (*e.g.*, Walrafen, 1962). The component C1 at ~3280 cm^{-1} is assigned to O–H stretching vibrations of strongly hydrogen-bonded, polymerised water species because the relative intensity of this component correlates with the dependence of polymerisation on pressure and temperature (*e.g.*, Sahle *et al.*, 2013) and decreases with addition of salt (*e.g.*, Walrafen, 1962).

In our experiments at 21 ± 1 °C, we obtained data for the ν_1-SO$_4^{2-}$ Raman shift of the SO$_4$* and CIP components (Figs. 1a and 1b), the abundance of contact ion pairs, as calculated from the relative integrated intensities of the CIP and SO$_4$* components (Fig. 1c), and the Raman shifts of the three band components in the O–H stretching region (Fig. 1d). At each studied concentration of 0.5, 1.7 and 2.0 molal MgSO$_4$, increasing pressure produces linear changes in the ν_1-SO$_4^{2-}$ Raman shift of SO$_4$* of ~6 cm^{-1}GPa^{-1} for the data to 0.17 GPa (Fig. 1a).

Above 0.7 GPa, the pressure dependence of that Raman shift is also linear and independent of composition, but the slope is shallower (~3 cm^{-1}GPa^{-1}). All data show systematic negative departures from linearity beginning at 0.17 GPa, which corresponds to the LDW-HDW transition (Fig. 1a) and agrees with a previous study on NaSO$_4$ solutions (Schmidt, 2009). Departures from linearity continue to ~0.6 GPa. Similar behaviour is observed in the Raman shift of the CIP component in the same pressure interval (Fig. 1b).
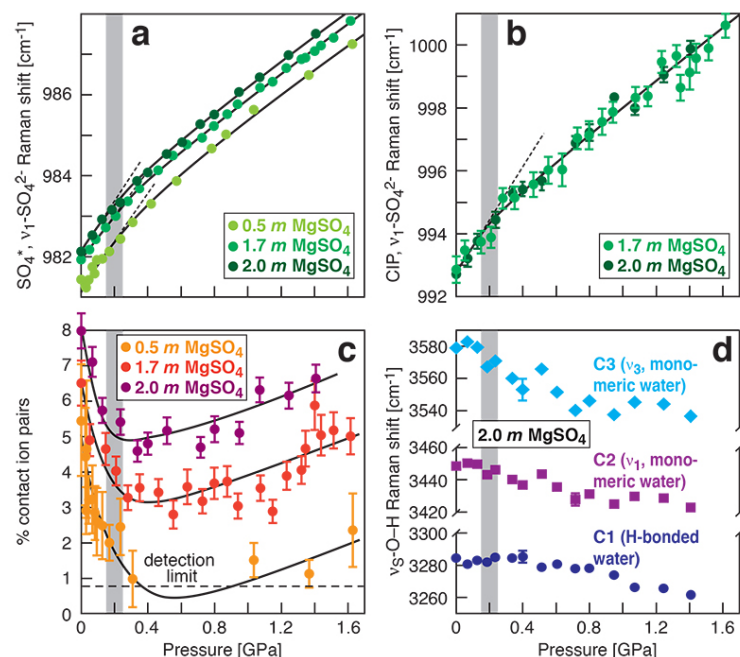

Figure 1 Raman spectroscopic results at 21 ± 1 °C as a function of pressure. The shadowed band is the pressure range of the LDW-HDW transition at about 20 °C (Fanetti *et al.*, 2014). **(a-b)** Raman shift ω of the v_1-SO$_4^{2-}$ mode of the SO$_4$* component (a) and of the CIP component (b). Dashed lines denote the $(\partial\omega/\partial P)_{T=21°C}$ slopes in cm^{-1}GPa^{-1} from linear fits of data at <0.17 GPa. **(c)** Percentage of contact ion pairs as a function of pressure at 21 °C. **(d)** Raman shift of fitted band components in the v_S-O–H region of the 2.0 molal MgSO$_4$ solution.

At 21 °C, the percentage of Mg^{2+}SO$_4^{2-}$(aq) CIP initially decreases with pressure along the isotherms at each concentration (Fig. 1c). Above ~0.4 GPa, however, it increases nearly linearly with rising pressure in 1.7 and 2.0 molal solutions. The 0.5 molal solution is consistent with this behaviour, although errors are larger and the abundance of CIPs is below the detection limit at about 0.4–0.9 GPa. This was not observed at 50–150 °C, where the percentage of CIP in 0.75 and 2.25 molal MgSO$_4$ solutions generally decreased with pressure along all
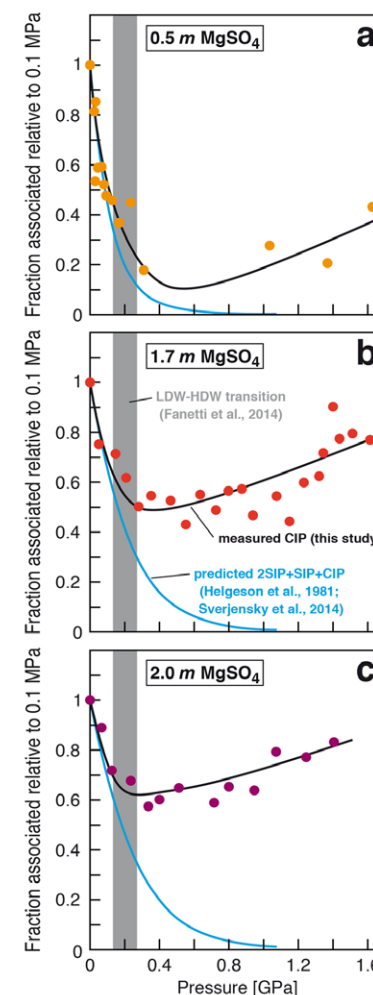
Figure 2 Fraction of MgSO$_4$ associated at 21 ± 1 °C relative to that at ambient pressure, as determined by Raman spectroscopy and thermodynamic modelling, for 0.5 **(a)**, 1.7 **(b)**, and 2 molal solutions **(c)**. Thick black lines are trend lines for the fraction of CIP from Raman spectroscopic data fit by eye. Blue lines denote the fraction of the sum of the CIP, SIP and 2SIP ion pairs calculated from a thermodynamic model based on the DEW model (Sverjensky *et al.*, 2014) and the Helgeson-Kirkham-Flowers ion activity model (Helgeson *et al.*, 1981). The comparison assumes that the proportionality between equilibrium constants associated with expelling the H$_2$O molecules between ions is constant and independent of pressure. This assumption yields a minimum difference in predicted and observed CIP. The shadowed band is the pressure range of the LDW-HDW transition at about 20 °C (Fanetti *et al.*, 2014).

isotherms (Fig. S-2). The data for the pressure dependence of the ν_S-O–H Raman shift for C1, C2 and C3 in the 2.0 molal solution generally suggest declining frequency with rising pressure (Fig. 1d), consistent with lengthening of the O–H-bonds and thus shorter hydrogen bonds between the water molecules. The scatter in these data is fairly large because the ν_S-O–H components are very broad and overlap (Fig. S-1b).

The finding of compression-enhanced contact ion pairing above ~0.2 GPa at 21 °C (Fig. 1c) is contrary to the predicted trend of increasing salt dissociation with pressure. Previous Raman spectroscopic and electrical conductivity studies (Ritzert and Franck, 1968; Chatterjee *et al.*, 1974) at less than about 0.5 GPa and near ambient temperatures indicated increasing dissociation of $MgSO_4$ in aqueous solution upon compression. Thermodynamic modelling also yields a continually increasing extent of ion pair dissociation with rising pressure, unaffected by the LDW-HDW transition (Fig. 2), but data used in such models are based on correlations and extrapolations typically derived from conductivity data at very different pressures and temperatures. The static dielectric constant of H_2O is a key parameter governing the extent of ion association in aqueous solutions; however, it does not decrease with increasing pressure in the HDW field (Fernandez *et al.*, 1995). Based on Coulomb's law, the observed increased contact ion pairing must therefore be caused by a decrease in the distance between cation and anion. An increasing tendency to form ion pairs with pressure can thus be related to increased hydrogen-bond breaking with pressure resulting in a collapsed second coordination shell in HDW (Soper and Ricci, 2000; Krisch *et al.*, 2002; Fanetti *et al.*, 2014). Therefore, the inferred relationship between water structure and ion pairing implies that significant interaction between ions and water exists at distances larger than the first shell, which has long been a matter of debate (*c.f.* Marcus, 2009).

Implications for Planetary Oceans and Interiors

Generally, the increase in ion pairing with pressure affects properties such as solubility, viscosity, sound absorption and electrical conductance. For a given salinity, isothermal salt re-association will yield lower ionic strength (and thus ion activity) than predicted from extrapolation of low-pressure behaviour, and also lower conductivity of deep ocean waters, which is relevant for the interpretation of spacecraft-based magnetometric data (*e.g.*, Hand and Chyba, 2007).

Our results show that high pressures and fairly low temperatures are required for pressure-induced ion pairing in salty water. In nature, it will therefore only occur in relatively large, cool planetary bodies with thick liquid water shells. Extrasolar ice planets may well meet these requirements, as well as some ocean planets such as Kepler-62e and -62f (Kaltenegger *et al.*, 2013). So too would cold, deep, aqueous planetary settings in our solar system, which include the interiors of Pluto and the largest icy moons of Jupiter and Saturn. There is considerable evidence for a subsurface ocean in Europa, but plausible basal ocean pressure is too low (Spohn and Schubert, 2003; Hand and Chyba, 2007) for salt
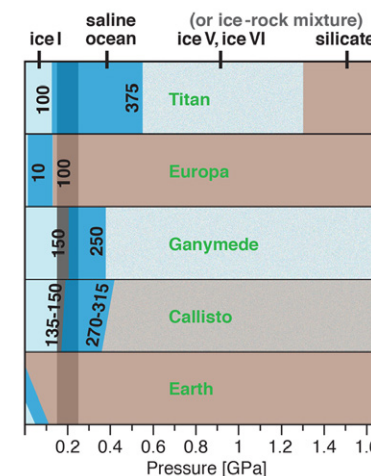
Figure 3 Comparison of models of the interiors of Titan (Tobie *et al.*, 2012), Europa (Spohn and Schubert, 2003; Hand and Chyba, 2007; Valenti *et al.*, 2012), Ganymede (Vance *et al.*, 2014; Saur *et al.*, 2015), and Callisto (Kuskov and Kronrod, 2005) with approximate depths of the subsurface ocean boundaries in km. The shadowed band is the pressure range of the LDW-HDW transition at about 20 °C (Fanetti *et al.*, 2014).

re-association (Fig. 3). However, Ganymede (Vance *et al.*, 2014; Saur *et al.*, 2015) and Saturn's moon Titan (Grasset and Pargamin, 2005; Tobie *et al.*, 2012) likely possess deep subsurface oceans with substantial portions of the liquid water column in the LDW-HDW transition region (Fig. 3). Deep ocean waters of Pluto, and an at least partly differentiated Callisto, would also exceed 0.2 GPa (Spohn and Schubert, 2003; Kuskov and Kronrod, 2005; Hammond *et al.*, 2016). As in Europa, the existence of a thick saline subsurface ocean in Callisto is indicated by a conductive layer at a depth of less than about 300 km inferred from magnetic field perturbations observed by the Galileo spacecraft (Zimmer *et al.*, 2000).

In this context, our finding of increasing ion association with pressure is important for understanding the coupled evolution of ocean salinity and the silicate interiors of the icy satellites. The salts of planetary oceans are acquired chiefly from sub-seafloor weathering reactions (Zolotov and Shock, 2001). About 75 % of the salts produced by low-temperature aqueous alteration of chondrite under oxidising conditions are magnesium sulphate hydrates (Hogenboom *et al.*, 1995). Thus, H_2O + $MgSO_4$ is one of the most relevant model systems for planetary oceans. Consumption of ions by ion pair formation via

$$Mg^{2+} + SO_4^{2-} = MgSO_4^0 \qquad \text{Eq. 1}$$
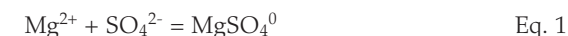
requires commensurate forward progress of any magnesium silicate weathering reactions, such as olivine:

$$Mg_2SiO_4 + 2H^+ = Mg^{2+} + 2SiO_2 + 2H_2O \qquad \text{Eq. 2}$$

Therefore, the greater extent of salt association in HDW pore waters beneath the ocean floors of large icy satellites will enhance the progress of dissolution reactions relative to expectations based on LDW. This will generate a more voluminous planetary reservoir of altered rock, and – when the pore fluids decompress upon delivery to the oceans – higher ocean salinities. A thick layer of high-pressure ices and hydrates on the floor of a deep cold subsurface ocean (Fig. 3) could decrease this effect, but dissolved salts would diminish such a layer. Ganymede might have a stack of several ocean layers separated by different phases of ice, with the lowest liquid layer adjacent to the rocky mantle below (Vance *et al.*, 2014).

Acknowledgements

Additional Information

Supplementary Information accompanies this letter at www.geochemicalperspectivesletters.org/article1707

Reprints and permission information is available online at http://www.geochemicalperspectivesletters.org/copyright-and-permissions

Cite this letter as: Schmidt, C., Manning, C.E. (2017) Pressure-induced ion pairing in MgSO$_4$ solutions: Implications for the oceans of icy worlds. *Geochem. Persp. Let.* 3, 66-74.

References

Chatterjee, R.M., Adams, W.A., Davis, A.R. (1974) A high-pressure laser Raman spectroscopic investigation of aqueous magnesium sulfate solutions. *Journal of Physical Chemistry* 78, 246–250.

Fanetti, S., Lapini, A., Pagli, M., Citroni, M., Di Donato, M., Scandolo, S., Righini, R., Bini, R. (2014) Structure and dynamics of low-density and high-density liquid water at high pressure. *Journal of Physical Chemistry Letters* 5, 235–240.

Fernandez, D.P., Mulev, Y., Goodwin, A.R.H., Levelt Sengers, J.M.H. (1995) A database for the static dielectric constant of water and steam. *Journal of Physical and Chemical Reference Data* 24, 33–53.

Grasset, O., Pargamin, J. (2005) The ammonia-water system at high pressures: Implications for the methane of Titan. *Planetary and Space Science* 53, 371–384.

Hammond, N.P., Barr, A.C., Parmentier, E.M. (2016) Recent tectonic activity on Pluto driven by phase changes in the ice shell. *Geophysical Research Letters* 43, 6775–6782.

Hand, K.P., Chyba, C.F. (2007) Empirical constraints on the salinity of the Europan ocean and implications for a thin ice shell. *Icarus* 189, 424–438.

Helgeson, H.C., Kirkham, D.H., Flowers, G.C. (1981) Theoretical prediction of the thermodynamic behavior of aqueous electrolytes at high pressures and temperatures. IV. Calculation of activity coefficients, osmotic coefficients, and apparent molal and standard and relative partial molal properties to 5 kb and 600 °C. *American Journal of Science* 281, 1241–1516.

Hogenboom, D.L., Kargel, J.S., Ganasan, J.P., Lee, L. (1995) Magnesium sulfate-water to 400 MPa using a novel piezometer: densities, phase-equilibria, and planetological implications. *Icarus* 115, 258–277.

Kaltenegger, L., Sasselov, D., Rugheimer, S. (2013) Water-planets in the habitable zone: Atmospheric chemistry, observable features, and the case of Kepler-62e and -62f. *Astrophysical Journal Letters* 775, L47.

Kawamoto, T., Ochiai, S., Kagi, H. (2004) Changes in the structure of water deduced from the pressure dependence of the Raman OH frequency. *Journal of Chemical Physics* 120, 5867–5870.

Krisch, M., Loubeyre, P., Ruocco, G., Sette, F., Cunsolo, A., D'Astuto, M., LeToullec, R., Lorenzen, M., Mermet, A., Monaco, G., Verbeni, R. (2002) Pressure evolution of the high-frequency sound velocity in liquid water. *Physical Review Letters* 89, 125502.

Kuskov, O.L., Kronrod, V.A. (2005) Internal structure of Europa and Callisto. *Icarus* 177, 550–569.

Li, F., Cui, C.L., He, Z., Cui, T., Zhang, J., Zhou, Q., Zou, G.T., Sasaki, S. (2005) High pressure-temperature Brillouin study of liquid water: Evidence of the structural transition from low-density water to high-density water. *Journal of Chemical Physics* 123, 174511.

Marcus, Y. (2009) Effect of ions on the structure of water. *Chemical Reviews* 109, 1346–1370.

Mirwald, P. (2005) Evidence of PVT anomaly boundaries of water at high pressure from compression and NaCl·2H$_2$O dehydration experiments. *Journal of Chemical Physics* 123, 124715.

Okhulkov, A.V., Demianets, Y.N., Gorbaty, Y.E. (1994) X-ray scattering in liquid water at pressures of up to 7.7 kbar: Test of a fluctuation model. *Journal of Chemical Physics* 100, 1578–1588.

Ritzert, G., Franck, E.U. (1968) Electrical conductivity of aqueous solutions at high temperatures and pressures. 1. KCl, BaCl$_2$, Ba(OH)$_2$ and MgSO$_4$ up to 750 °C and 6 kbar. *Berichte der Bunsengesellschaft für physikalische Chemie* 72, 798–808.

Rudolph, W.W., Irmer, G., Hefter, G.T. (2003) Raman spectroscopic investigation of speciation in MgSO$_{4(aq)}$. *Physical Chemistry Chemical Physics* 5, 5253–5261.

Sahle, C., Sternemann, C., Schmidt, C., Lehtola, S., Jahn, S., Simonelli, L., Huotari, S., Hakala, M., Pylkkänen, T., Nyrow, A., Mende, K., Tolan, M., Hämäläinen, K., Wilke, M. (2013) Microscopic structure of water at elevated pressures and temperatures. *Proceedings of the National Academy of Sciences of the United States of America* 110, 6301–6306.

Saur, J., Duling, S., Roth, L., Jia, X., Strobel, D.F., Feldman, P.D., Christensen, U.R., Retherford, K.D., McGrath, M.A., Musacchio, F., Wennmacher, A., Neubauer, F.M., Simon, S., Hartkorn, O. (2015) The search for a subsurface ocean in Ganymede with Hubble Space Telescope observations of its auroral ovals. *Journal of Geophysical Research* 120, 1715–1737.

Schmidt, C. (2009) Raman spectroscopic study of a H$_2$O + Na$_2$SO$_4$ solution at 21–600 °C and 0.1 MPa to 1.1 GPa: Relative differential ν_1-SO$_4^{2-}$ Raman scattering cross sections and evidence of the liquid–liquid transition. *Geochimica et Cosmochimica Acta* 73, 425–437.

Soper, A.K., Ricci, M.A. (2000) Structures of high-density and low-density water. *Physical Review Letters* 84, 2881–2884.

Spohn, T., Schubert, G. (2003) Oceans in the icy Galilean satellites of Jupiter? *Icarus* 161, 456–467.

Sverjensky, D.A., Harrison, B., Azzolini, D. (2014) Water in the deep Earth: The dielectric constant and the solubilities of quartz and corundum to 60 kb and 1200 °C. *Geochimica et Cosmochimica Acta* 129, 125–145.

TOBIE, G., GAUTIER, D., HERSANT, F. (2012) Titan's bulk composition constrained by Cassini-Huygens: implication for internal outgassing. *Astrophysical Journal* 752, 125.

VALENTI, P., BODNAR, R.J., SCHMIDT, C. (2012) Experimental determination of H_2O–NaCl liquidi to 25 mass% NaCl and 1.4 GPa: Application to the Jovian satellite Europa. *Geochimica et Cosmochimica Acta* 92, 117–128.

VANCE, S., BOUFFARD, M., CHOUKROUN, M., SOTIN, C. (2014) Ganymede's internal structure including thermodynamics of magnesium sulfate oceans in contact with ice. *Planetary and Space Science* 96, 62–70.

WALRAFEN, G.E. (1962) Raman spectral studies of the effects of electrolytes on water structure. *Journal of Chemical Physics* 36, 1035–1042.

ZIMMER, C., KHURANA, K.K., KIVELSON, M.G. (2000) Subsurface oceans on Europa and Callisto: Constraints from Galileo magnetometer observations. *Icarus* 147, 329–347.

ZOLOTOV, M.Y., SHOCK, E.L. (2001) Composition and stability of salts on the surface of Europa and their oceanic origin. *Journal of Geophysical Research* 106, 32815–32827.